한국정밀공학회지 제 39 권 제 3 호 pp. 201-208 March 2022 / 201
J. Korean Soc. Precis. Eng., Vol. 39, No. 3, pp. 201-208 http://doi.org/10.7736/JKSPE.021.115
ISSN 1225-9071 (Print) / 2287-8769 (Online)

토사 분포를 고려한 모터 그레이더 블레이드 로테이션 제어 전략

Strategy for Motor Grader Blade Rotation considering Soil Distribution

이진규[1], 배장호[2], 권오영[1], 김한얼[1], 채솔[1], 홍대희[3,#]
Jinkyu Lee[1], Jangho Bae[2], Oyoung Kwon[1], Hanul Kim[1], Chai Sol[1], and Daehie Hong[3,#]

1 고려대학교 대학원 기계공학과 (Department of Mechanical Engineering, Graduate School, Korea University)
2 경성대학교 기계자동차공학과 (Department of Mechanical and Automotive Engineering, Kyungsung University)
3 고려대학교 기계공학부 (School of Mechanical Engineering, Korea University)
Corresponding Author / E-mail: dhhong@korea.ac.kr, TEL: +82-2-3290-3369
ORCID: 0000-0002-2773-2629

KEYWORDS: Motor grader (모터 그레이더), Blade rotation (블레이드 로테이션), Recurdyn (리커다인), EDEM (이디이엠), Co-Simulation (합동 시뮬레이션), Work quality (일 효율)

Research on the automation of many types of construction equipment, including motor graders, is being actively conducted. In a motor grader cabin, the operator has difficulty observing the working environment because of a constructed field of view. Thus, workers rely on their experience and senses. Further, the working environment of the blade must be observed, and a control algorithm should be created to enable autonomous operation. In this study, a blade rotation control strategy considering the soil distribution was proposed. First, a co-simulation environment was constructed using RecurDyn for multibody dynamics analysis and EDEM for discrete element method simulation, and simulations were performed to determine the correlation between soil distribution and the blade rotation angle. Work quality and blade load were analyzed according to the simulation results. The optimal blade rotation angle according to soil distribution was obtained to develop the strategy for autonomous flattening and scattering work. The proposed control strategy was implemented in a 1/4 full-scale motor grader experimental setup. An experiment to evaluate work quality was conducted to validate the effectiveness of the proposed methods. The experimental results indicated that the proposed strategy effectively performed scattering work.

Manuscript received: November 10, 2021 / Revised: January 4, 2022 / Accepted: February 7, 2022

1. Introduction

A motor grader is construction equipment that can perform various tasks on a construction site. The functions of motor graders include flattening, scraping slope, and ditching. Flattening is the process of flattening the soil to a desired height using a blade. Scraping slope is used to make a slope wherein the blade is pulled out to the side. Meanwhile, ditching is a process of making drainage channels on both sides of the road. Among them, the common function of motor graders is soil flattening. To flatten the soil with a blade, the distribution of the soil around the blade should be determined. However, the driver on the driver's seat has narrow visibility [1]. Further, there is no technology to monitor the soil around the motor grader blades. Thus, research on improving work quality through blade rotation control and fully autonomous blade control has not been conducted thus far. In addition, the concentration of load due to the inclination of the soil during work may stress the hydraulic cylinder or damage the blade [2]. Therefore, ensuring that the load is not concentrated on the blade is crucial.

Among the degrees of freedom of movement of the motor grader blades, there are studies that automatically control lifting [3]. They aim to maintain the desired height during work using a laser transmitter and receiver. One study also measured the position and angle of the blade using RTK-GNSS [4]. This study

established a technology that automatically maintains the lifting and lowering of the blade, but has difficulty working autonomously according to soil distribution; hence, autonomous operation of blade rotation and tilt is impossible. A study on the relationship between the rotation angle of the blade and the cross slope of the road has been conducted also [5]. Their results reveal the influence of various angles of the blade and the factors that determine the cross slope, but does not know the criteria for autonomous operation of blade rotation. Therefore, the soil distribution and blade rotation angle should be simulated to determine the rotation control algorithm.

To determine the rotation control algorithm, multibody dynamics (MBD) and discrete element method (DEM) simulations were conducted. In particular, sand was made in DEM software. DEM for soil-implement interaction has been used by several researchers (such as Oida, et al.) [6] to model a shoe-soil interaction and for the interaction between soil and a vibrating subsoiler (Tanaka, et al.) [7]. A 2D and 3D model of filling dragline buckets was reported by Cleary [8] and Loughran, et al. [9], respectively. This model has also been used to develop a calibrated DEM plow model to examine the effects of width, speed, and depth on tillage forces and furrow profiles [10]. Other uses of DEM include theoretical foundation and practical support for loaders automatically scooping intelligent resistance reduction [11].

DEM can be used together with MBD and CAE for dynamic analysis of mechanical devices [12]. Others use DEM with MBD to optimize heavy equipment for handling bulk materials [13]. Through co-simulation of MBD and DEM, a situation was created in which the motor grader blade pushes through the soil.

In this study, blade rotation control algorithm of considering the soil distribution is proposed. First, a simulation was performed to analyze the correlation between the soil distribution and blade rotation angle through the co-simulation of RecurDyn and EDEM. The soil distribution was distributed according to the blade position, and the blade rotation angle was classified into three categories. After analyzing the work quality and blade load according to simulation results, the algorithm was developed by analyzing the optimal blade rotation angle according to soil distribution and built an algorithm. Subsequently, a motor grader experimental device with a length 2 m was manufactured to recognize the soil distribution. The Intel Realsense D455 camera was placed between the front wheels to record the working environment around the blade. The soil distribution recognition program uses OpenCV to determine where large amounts of soil have accumulated. The experimental device is composed of a steering part, a driving part, a grader blade, three linear actuators and a BLDC motor to control the degree of freedom of the blade. The simulation site similar to the road construction site was made using experimental equipment and the algorithm was verified using real soil.

The remainder of this paper is organized as follows. Section 2 explains the co-simulation of RecurDyn, EDEM and the algorithm. Section 3 describes the field experiments. Section 4 evaluates the results of the field experiment and verifies the algorithm. Section 5 concludes with a summary of this study.

2. MBD-DEM Co-Simulation

2.1 Multibody Dynamics (MBD)

RecurDyn was used as MBD program. RecurDyn is a computer-aided engineering (CAE) software that can analyze both rigid and flexible bodies and is fast and efficient. In simulation, RecurDyn was used for creating the motor grader blades and the testbed floor. The bottom surface was created to be sufficiently wide for the blade. A space of at least 10 m was provided for the blade to work. The blade has a length of 4 m to match the size of the actual motor grader. The movement speed of the blade was set to 1 m/s, and the rotation angles were set to 15, 30, and 45° according to each experiment.

The coefficient settings for the simulation are listed in Table 1. The most important setting factors in RecurDyn are the contact characteristics. The stiffness coefficient was set to 10,000. If the stiffness coefficient is set to be quite small, equilibrium is achieved only when the displacement is quite large. Because displacement should not exist, the stiffness coefficient must be sufficiently large. Conversely, if the stiffness coefficient is quite large, the force changes rapidly, which may adversely affect the analysis stability. Subsequently, the damping coefficient was set to 10,000. For friction, the static threshold velocity was set to 1, the dynamic threshold velocity to 1.5, and the static friction coefficient to 0.37.

2.2 Discrete Element Method (DEM)

In recent years, several simulation approaches have become possible with the development of computer technology. DEM simulation is an analysis technique that starts with molecular

Table 1 MBD parameters

Parameter	Value
Stiffness coefficient	10,000
Damping coefficient	10,000
Static threshold velocity [m/s]	1
Dynamic threshold velocity [m/s]	1.5
Static friction coefficient	0.37

Table 2 DEM parameters

Parameter	Value	Reference
Particle shape	Sphere	14
Poisson's ratio	0.32	15
Solid density [kg/m^3]	2650	16
Shear modulus [Pa]	2.26e+07	15
Soil-soil interaction		
Coefficient of restitution	0.01	17
Coefficient of static friction	0.49	15
Coefficient of rolling friction	0.5	15
Soil-tool interaction		
Coefficient of restitution	0.01	17
Coefficient of static friction	0.37	15
Coefficient of rolling friction	0.05	18

dynamics and is a method of simulating discrete matter. The DEM calculates the trajectory of each particle and predicts the behavior of the BULK as the overall sum of the particle behaviors. This technique is different from continuum-based FEM, which simultaneously shows the characteristics of solids and fluids using granular materials. The DEM can numerically calculate finite particle displacements and rotations. In addition, it can automatically perform contact detection for the assembly of particles.

EDEM was used as DEM simulation program. EDEM is a program developed by DEM Solutions Ltd. (Edinburgh, Scotland, UK) for handling bulk materials. EDEM 2020 was worked on a computer with Intel (R) Core (TM) i7-4790K COU @ 4.00 GHz and 32 GB RAM. Several steps are followed for the DEM simulation. First, set the particles to be used in the simulation and their properties. The set values include particle size, shape, Poisson's ratio, density, shear modulus, and Young's modulus. Coefficients for the interactions between particles and between particles and tools were set. The set values include the coefficient of restitution, a coefficient of static friction, and a coefficient of rolling friction.

In this simulation, the EDEM was used to generate the soil model. The soil on which motor graders work was mostly sand. Therefore, the sand particles and the coefficients for their interactions should be determined as presented in Table 2 [18].

2.3 Co-Simulation

In this study, MBD and DEM were co-simulated to simulate the operation of motor grader blades. Steps involved in the MBD-DEM co-simulation are as followed. 1) The ground and blade shapes were created using RecurDyn. After adjusting all the necessary settings, the solid files that required to be co-simulated as wall files were saved and were then exported to complete the MBD preparation. 2) The exported wall files were loaded into EDEM. A particle model was created to match it. All the necessary settings were adjusted, and the coupling server was turned on. 3) Finally, the two programs were co-simulated, and the results were verified and analyzed by each program.

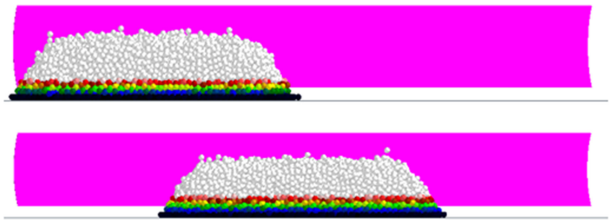

Fig. 1 Soil distribution: (From up to bottom) Soil on the left side, soil on the middle side

2.4 Simulation Setup

The MBD-DEM co-simulation was conducted for scattering and flattening. The scattering operation was carried out by dividing the location of the soil into two parts: one focused on one side of the blade and one focused on the middle of the blade. The flattening was carried out with the soil spread evenly. In each case, the blade rotation angle was divided into 15, 30, and 45°. The first scattering operation occurs when the soil is mainly accumulated on the left side of the blade as shown in Fig. 1. The number of particles in the soil was 50,000, and the simulation was prepared by pouring the soil from a dump truck. The second scattering operation occurs when the soil is gathered in the middle of the blade as shown in Fig. 1. A simulation was created and blade rotation angle was changed.

Finally, the flattening process evenly spreads the soil to the desired height. As the scattering work is finished, the soil is spread widely, and the number of particles is 60,000.

2.5 Simulation Results

Fig. 2 shows the simulation results of the scattering and flattening work. This is the simulation result of the flattening work that spreads the soil evenly to the desired height. The simulation results were evaluated in terms of work quality and stability. The work quality was compared to the difference between the desired height and the height of the simulation result [19]. Stability was evaluated by comparing the forces acting on the blades during operation. Table 3 shows the simulation results. Work quality showed similar results for all three angles. However, stability received less load as the angle increased. Therefore, setting the blade rotation angle to 45° is crucial for the grading operation for the highest stability.

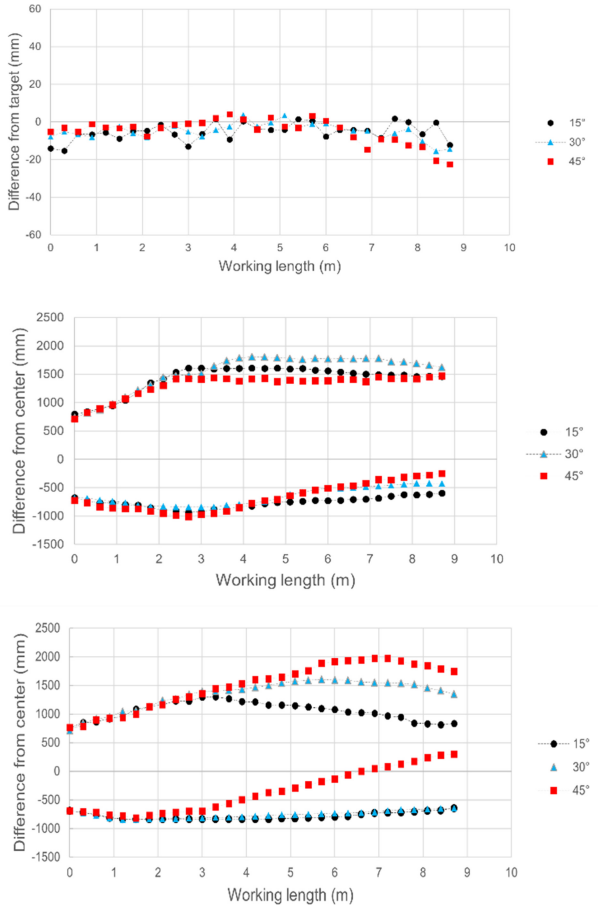

Fig. 2 Simulation results: (From up to bottom) Flattening work, scattering work (Soil on the left side), and scattering work (Soil on the middle side)

The simulation results were evaluated in terms of work quality and stability. Work quality was evaluated by measuring the left and right distances of the soil to evaluate its spread. We considered the center of the soil to be 0 and measured the spread to the left and right. Stability was evaluated by comparing the forces acting on the blades during operation. Work quality was best at 30° as shown in Table 3. The stability was similar for all three angles. In the case of 30°, the work quality is good by about 15% compared to the rest. Therefore, setting the blade rotation angle to 30° is crucial when the soil is mainly accumulated on the left side of the blade.

This is the simulation result of the scattering work in which the soil is gathered in the middle of the blade. The evaluation was performed as described previously. Work quality was best at 15° as shown in Table 3. The stability was similar for all three angles. In the case of 15°, the work quality is good by about 10% compared to the rest. Therefore, setting the blade rotation angle to 15° is crucial when the soil is gathered in the middle of the blade. Productivity is mainly considered in the process of finding the optimal blade angle, so productivity is also mainly considered in the field test.

Table 3 Simulation results

	15°	30°	45°
Flattening work			
Height difference [mm]	-5.3	-4.8	-4.9
Blade load [N]	679.1	607.3	511.1
Scattering work (Left)			
Degree of spread [mm]	1,833.9	2,104.8	1,854.2
Blade load [N]	1,154.5	1,144.7	1,144.1
Scattering work (Middle)			
Degree of spread [mm]	2,190.5	2,081.9	1,981.4
Blade load [N]	1,207.1	1,173.1	1,147.3

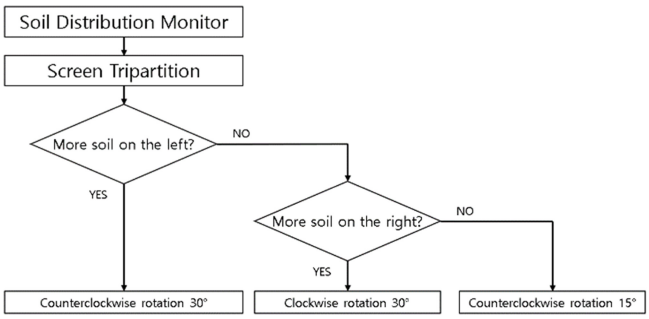

Fig. 3 Blade rotation control algorithm

2.6 Blade Rotation Control Algorithm

Blade rotation control algorithm was created based on the simulation results. The algorithm was constructed as shown in Fig. 3. First, the soil distribution was measured. Recognizing the distribution of soil was accomplished using the techniques discussed in Section 3.2. When the distribution of soil is known, the blade rotation angle is controlled according to the simulation results. The Dynamixel wizard 2.0 program was used to control the blade rotation angle. If the soil is concentrated on the left side of the blade, the blade is rotated 30° counterclockwise. Otherwise, if there is a lot of soil on the right side of the blade, the blade is rotated 30° clockwise. In both cases, if the soil is concentrated in the center of the blade, the blade is rotated 15° counterclockwise. Based on the simulation results, an algorithm that can control the blade rotation angle by recognizing the distribution of soil was built. This algorithm is verified through field experiments with actual motor grader experimental equipment in Section 4.

3. Field Experiments

3.1 Motor Grader Experimental Setup

To verify the results obtained through the previous simulation, a

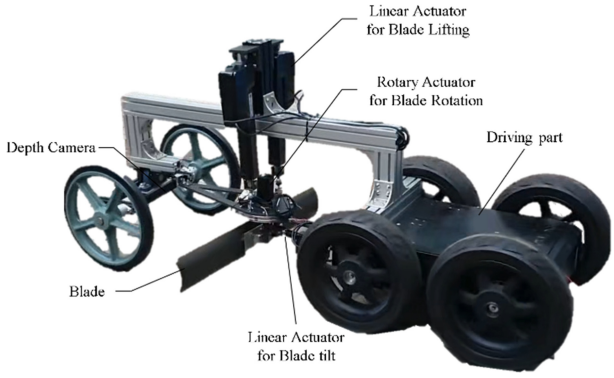

Fig. 4 Overview of motor grader experimental equipment

motor grader experimental device was developed (Fig. 4). The experimental device is about 1/4 scale of the actual motor grader, and the length is 2, the body width is 0.75, the height is 0.9, and the blade length is 1 m. The blade of the motor grader has several degrees of freedom. It was designed to be similar to the actual motor grader and designed to enable blade lifting, rotation, and tilt among several degrees of freedom. First, for blade lifting, two Thompson Electrak HD linear actuator were used. The maximum weight was 1,700 N, the maximum stroke was 300 mm, and the CAN bus J1939 was provided. For the blade tilt, a Thompson Electrak MD linear actuator was used. The maximum weight is 500 N, the maximum stroke is 100 mm, and the CAN bus J1939 is provided. For blade rotation, Robotis PH54-200-S500-R was used. The operating torque was 44.7 Nm, the maximum rotation speed was 29 rpm, and RS485 multi-drop bus was provided.

3.2 Soil Distribution Recognition Method

A depth camera was installed in the experimental device to monitor the soil accumulated in front of the blade during motor grader work. It was installed between the front wheels, where the angle of view of the camera can capture the entire blade. Intel's RealSense D455 camera was used as the depth camera. The depth field of view was 87 × 58°, the RGB sensor field of view was 90 × 65°, the RGB frame resolution was 1,280 × 800, and the camera provided depth and RGB data.

Using the RGB data obtained from the depth camera, OpenCV is used to create an algorithm to judge the soil distribution [20]. First, in the image, the blade is divided into three parts: Left, middle, and right. The brightness of the image was adjusted and a bidirectional filter was used. The image color was changed to HSV color space and make the h range 0 to 12 and s and v 0 to 100%. Thus, only the soil part can be recognized in the image as shown in Fig. 5. Then, Otsu binarization was performed and find the contour with the largest area. Next, the contour shape is defined through contour approximation, and the area where the soil has accumulated the most is indicated by comparing the contour areas of each part (Fig. 5).

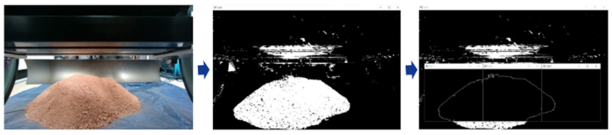

Fig. 5 Soil distribution recognition method: (From left to right) Original image, only soil detection, three-part soil distribution detection

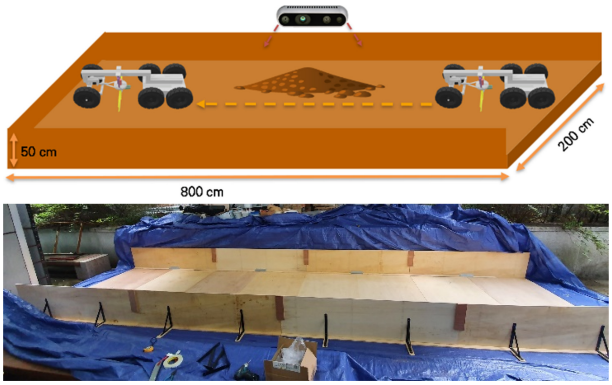

Fig. 6 Field test bed: (From up to bottom) Overview of field test, field test bed

3.3 Field Experiment Configuration

As shown in Fig. 6, a field test bed of 8 m in length, 2 m in width, and 0.5 m in height was constructed. The sides and undersides were made of plywood. Desired soil distribution was created in the test bed and the experiment was conducted with the motor grader experimental equipment. The soil distribution for the flattening work and scattering work was positioned as shown in Fig. 6. The soil distribution for the flattening work was made of a pile of soil with a length of 2, width of 0.75, and height of 0.25 m. The soil distribution for the scattering work was made with a pile of soil with a length of 1 m, width of 0.5, and height of 0.3 m. Both tasks made the environment identical to the simulation. The speed of the motor grader was 1 m/s and it was run at the same speed as in the simulation.

In the field test, a flattening experiment was performed to confirm that the experimental results were reasonable. Three cases of 15, 30, and 45° were tested with the same pile of soil. The experimental results were compared with the target distance by measuring the depth data of the flattened part of the soil and averaging it. Experimental images were taken from the top using Inter's RealSense D455 to implement the top view.

A scattering experiment was performed to verify that the algorithm built through the simulation results was reasonable. The

Table 4 Field experiments results

#	1	2	3	4	5	Average
Flattening work						
Height difference with blade rotation 15° [mm]	-4.2	-4.5	-3.3	-2.1	-3.5	-3.5
Height difference with blade rotation 30° [mm]	-5.6	-4.5	-7.4	-7.8	-6.5	-6.4
Height difference with blade rotation 45° [mm]	-3.2	-2.6	-2.4	-2.2	-2	-2.5
Scattering work (Soil on left side)						
Degree of spread with blade rotation 15° [mm]	458.2	450.1	452.9	446.5	451.2	451.8
Degree of spread with blade rotation 30° [mm]	523.8	530.4	528	524.3	520.1	525.3
Degree of spread with blade rotation 45° [mm]	461.5	467.5	459.2	470.1	461.4	463.9
Scattering work (Soil on middle side)						
Degree of spread with blade rotation 15° [mm]	548.4	551.7	553.6	548.3	555.2	551.4
Degree of spread with blade rotation 30° [mm]	521.4	516.3	522.4	514.8	512.9	517.6
Degree of spread with blade rotation 45° [mm]	498.6	507.1	501.6	496	497.2	500.1

experiment was conducted by dividing the case where the soil was concentrated on the left side of the blade and the case where the soil was concentrated in the center for the scattering work experiment. As with the flattening work, the experiment was performed five times in three cases: 15, 30, and 45°. Similar to the simulation results, the experimental results were compared for the spread of the soil. Experimental images of the top view were taken. The degree of soil spread was compared by measuring the left and right distances of the soil and averaging the five experiments.

4. Experiment Results

4.1 Field Experiments

First, the results of the flattening work were analyzed to confirm that the experimental results were reasonable. The depth data of the part where the flattening work was performed were measured and compared. As shown in Table 4, the results are almost consistent with the target distance. This is consistent with the simulation results. Therefore, this experiment was reasonable.

The scattering operation experiment was conducted five times for each case. When the soil is concentrated on the left side of the blade, the average distance of the soil spread is 451.8 mm at 15°, 525.3 mm at 30°, and 463.9 mm at 45°. As shown in Table 4, 30° is the most efficient. As the basic working angle is 45°, the soil was spread 16% wider than in the basic working case. Thus, it has been shown that it is reasonable to rotate the blade by 30° if the soil is concentrated to the left of the blade.

In case the soil is concentrated in the middle of the blade, the average distance of the soil spread is 551.4 mm at 15°, 517.6 mm at 30°, and 500.1 mm at 45°. As shown in Table 4, 15° was the most efficient. As the basic working angle is 45°, the soil was spread 10% wider than in the basic working case. Thus, it has been shown that it is reasonable to rotate the blade by 15° if the soil is concentrated in the center of the blade.

Therefore, it was proved through actual field tests that the algorithm built through the simulation results was reasonable. Field test results were obtained similar to simulation results. The rationality of the experiment was demonstrated through a flattening work experiment, and the rationality of the algorithm is shown.

5. Conclusions

As research on the automation of heavy equipment used in construction sites has progressed, the number of research on autonomous operation and driving of motor graders is also increasing. Most motor graders work with blades, but the view from the driver's seat is narrow and requires instructions from many outside workers. Therefore, for the autonomous operation of the motor grader, it is necessary to monitor the soil around the blade and use it to control the blade. Currently, no study has been conducted to control the blade height. Therefore, this study attempted to control the blade rotation angle. In addition, the soil around the blades during work was monitored and an algorithm is proposed to determine where a large amount of soil is piled up and accordingly control blade rotation angle.

A MBD-DEM co-simulation was performed to create the blade rotation control algorithm. RecurDyn was used as MBD program and made the blade and floor. Then, EDEM was used as DEM program to create the desired shape of the soil. The simulation was

divided into flattening and scattering work, and the scattering operation was carried out by changing the location where the soil was accumulated. In each case, the optimal blade rotation angle is determined. A rotation angle control algorithm based on the soil distribution was built.

To verify the built algorithm, a motor grader experiment equipment and a field experiment test bed were produced. The motor grader experiment equipment was manufactured on a 1/4 scale of the actual motor grader. To verify the algorithm, experiments according to each soil shape were carried out five times. The flattening work showed a similar stability depending on the angle. In the case of scattering operation, when the soil is concentrated on one side, the case where the algorithm is applied showed approximately 16% better results. When the soil is concentrated at the center, the case where the algorithm is applied spreads the soil more widely by approximately 10%. This shows that the algorithm worked properly to increase the working quality of the motor grader.

Further research can be conducted to create an integrated blade autonomous working system. Currently, only each degree of freedom of the blade is capable of autonomous operation. If a working space is given, the desired soil leveling work can be performed by controlling all degrees of freedom to stack the soil at the desired height. In addition, by adding autonomous driving technology, a motor grader that can simultaneously move the workspace by itself and work autonomously should be developed.

ACKNOWLEDGEMENT

This work is supported by the Korea Agency for Infrastructure Technology Advancement (KAIA) grant funded by the Ministry of Land, Infrastructure and Transport (No. 20SMIP-A157130-01).

REFERENCES

1. Steele, J. (2006). Final report–blind area study for large mining equipment. (NIOSH Contract Report). https://www.cdc.gov/niosh/topics/highwayworkzones/bad/pdfs/BASFinalReport.pdf
2. Sakai, Y. (2002). Development of combined automatic blade control for snow-removing grader. KOMATSU. https://www.komatsu.jp/en/company/tech-innovation/report/pdf/150-02_E.pdf
3. Essaki, Y., Chiba, J., Funabashi, T., & Hayakawa, S., (1982). Automatic blade controls for earthmoving machines. SAE Technical Paper, 820640. https://doi.org/10.4271/820640
4. Serrano, L. (2013). Carrier-phase multipath mitigation in RTK-based GNSS dual-antenna systems. Ph.D. Thesis, University of New Brunswick.
5. Korytov, M., Shcherbakov, V., & Titenko, V., (2019). Effect of the angles of the earth-moving machine moldboard on the cross slope of the graded surface. In the Journal of Physics: Conference Series, 012070. https://doi.org/10.1088/1742-6596/1210/1/012070
6. Oida, A., Schwanghart, H., Ohkubo, S., & Yamazaki, M., (1997). Simulation of soil deformation under a track shoe by the DEM. In the 7th European Conference of ISTVS, 162.
7. Tanaka, H., Oida, A., Daikoku, M., Inooku, K., Sumikawa, O., et al., (2007). DEM simulation of soil loosening process caused by a vibrating subsoiler. 9, 5-10.
8. McBride, W., Sinnott, M., & Cleary, P., (2011). Discrete element modelling of a bucket elevator head pulley transition zone. Granular Matter, 13(2), 169-174. https://doi.org/10.1007/s10035-010-0243-2
9. Loughran, J., & Kannapiran, A., (2005). Three-dimensional simulation of the rolling of a saturated fibro-porous media. Finite Elements in Analysis and Design, 42(1), 90-104. https://doi.org/10.1016/j.finel.2005.05.006
10. Ucgul, M., & Saunders, C., (2020). Simulation of tillage forces and furrow profile during soil-mouldboard plough interaction using discrete element modelling. Biosystems Engineering, 190, 58-70. https://doi.org/10.1016/j.biosystemseng.2019.11.022
11. Chen, Y. H., Wang, J. Z., & Zheng, T., (2018). Simulation study on the scooping trajectories of loader based on EDEM. In the IOP Conference Series: Materials Science and Engineering, 042016. https://doi.org/10.1088/1757-899X/382/4/042016
12. Lai, Q., Yu, Q., & Dong, J., (2019). Dynamic analysis of rotary tiller gearbox based on EDEM, ADAMS and ANSYS. Journal of Intelligent & Fuzzy Systems, 36(2) 1153-1160. https://doi.org/10.3233/JIFS-169889
13. Curry, D., & Deng, Y., (2016). Optimizing heavy equipment for handling bulk materials with Adams-EDEM co-simulation. In the International Conference on Discrete Element Methods, 1219-1224. https://doi.org/10.1007/978-981-10-1926-5_126
14. Asaf, Z., Rubinstein, D., & Shmulevich, I., (2006). Evaluation of link-track performances using DEM. Journal of Terramechanics, 43(2), 141-161. https://doi.org/10.1016/j.jterra.2004.10.004
15. Tekeste, M., Tollner, E., Raper, R., Way, T., & Johnson, C., (2009). Non-linear finite element analysis of cone penetration in layered sandy loam soil-considering precompression stress state. Journal of Terramechanics, 46(5), 229-239. https://doi.org/10.1016/j.jterra.2009.05.005
16. Mousaviraad, M., Tekeste, M. Z., & Rosentrater, K. A., (2017). Calibration and validation of a discrete element model of corn using grain flow simulation in a commercial screw grain auger. Transactions of the ASABE, 60(4), 1403. https://doi.org/

10.13031/trans.12200

17. Tekeste, M. Z., Balvanz, L. R., Hatfield, J. L., & Ghorbani, S., (2019). Discrete element modeling of cultivator sweep-to-soil interaction: Worn and hardened edges effects on soil-tool forces and soil flow. Journal of Terramechanics, 82, 1-11. https://doi.org/10.1016/j.jterra.2018.11.001

18. Tekeste, M. Z., Way, T. R., Syed, Z., & Schafer, R. L., (2020). Modeling soil-bulldozer blade interaction using the discrete element method (DEM). Journal of Terramechanics, Vol. 88, pp. 41-52. https://doi.org/10.1016/j.jterra.2019.12.003

19. Hashimoto, T., & Fujino, K., (2019). Comparative study of experienced and inexperienced operators with auto-controlled construction machine. In the International Symposium on Automation and Robotics in Construction, 658-664. https://doi.org/10.22260/ISARC2019/0088

20. Kim, G. H., Park, M. S., Kim, D. Y., Lee, S. Y., & Lee, E. S., (2016). A method of wood section measuring and the image calibration using line laser. Journal of the Korean Society for Precision Engineering, 33(8), 641-646. https://doi.org/10.7736/KSPE.2016.33.8.641

Jinkyu Lee
M.S. candidate in the Department of Mechanical Engineering, Korea University. His research interests include field robotics.
E-mail: gg02064@korea.ac.kr

Jangho Bae
Professor in the Department of Mechanical and Automotive Engineering at Kyungsung University. His research interests include hydraulic robotic systems, human-robot collaboration systems and field robotics.
E-mail: janghobae@korea.ac.kr

Oyoung Kwon
Ph.D. candidate in the Department of Mechanical Engineering, Korea University. His research interests include smart manufacturing and field robotics.
E-mail: kdanny5445@korea.ac.kr

Hanul Kim
M.S. candidate in the Department of Automotive Convergence, Korea University. His research interests focus on electronic stability control.
E-mail: khanul@korea.ac.kr

Chai Sol
M.S. candidate in the Department of Mechanical Engineering, Korea University. His research interests include construction robot and laser machining tools.
E-mail: sol269012@gmail.com

Daehie Hong
Professor in the school of Mechanical Engineering, Korea University. His research interests include manufacturing automation, precision machine design and control, and field robotics.
E-mail: dhhong@korea.ac.kr